

# The Sideband Instability and the Onset of Wave Breaking

J.S.Reid  
CSIRO  
Division of Oceanography  
Hobart  
Tasmania

## Abstract

Packets of surface gravity waves of constant frequency and similar raised cosine envelopes were generated with a variety of amplitudes by means of a hydraulic paddle. The behaviour of each packet was observed with two capacitance probes, one near the paddle and the other some distance along the tank. In the time domain each packet was observed to evolve into a single envelope soliton and a "tail" as it travelled down the tank. In the frequency domain the initial spectral peak was observed to split into two peaks at frequencies on either side of the initial frequency in accordance with the well known "sideband" instability. In addition, for packets in excess of a particular threshold, wave breaking also occurred. The sideband instability was observed at amplitudes both above and below the threshold of breaking. At amplitudes below the threshold, energy was partitioned almost equally between the upper and lower sidebands but with the onset of breaking a smaller fraction of the initial energy was transferred to the upper sideband. The spectral behaviour of these evolving wave packets shows a number of features in common with that of wind waves observed in the open sea.

## Introduction

Much of the work on instabilities of surface gravity waves has ignored the phenomenon of wave breaking. The aim of this study was to set up a very simple tank experiment involving a nonlinear instability so as to examine the effect of breaking on the instability. Rather than set up a continuous periodic wave train, only isolated packets of waves were used in the belief that periodicity introduces an unnecessary constraint on a dynamical system, one not commonly encountered in nature.

## Experimental Setup

These experiments were conducted in the wave tank at the Australian Maritime College in Launceston Tasmania. The tank was 60m long, 3.5m wide and 1.5m deep. At one end was a hydraulically powered paddle hinged at the bottom of the tank

M. L. Banner, R. H. J. Grimshaw (Eds.)  
Breaking Waves  
IUTAM Symposium Sydney/Australia 1991  
© Springer-Verlag Berlin Heidelberg 1992

and driven by the output signal from a digital to analogue converter. At the other end was a sloping beach to help suppress reflections. Two capacitance probes, (termed "near" and "far"), were set up in the tank, at distances of 4.4m and 34.4m from the paddle respectively.

The computer driving the digital to analogue converter was programmed to generate a wave packet,  $V(t)$ , of the form

$$V(t) = 0.5 [1 - \cos(\omega_e t)] \sin(\omega_1 t) \quad (1)$$

in the range  $0 \leq t \leq t_e$  where  $t_e = 2\pi/\omega_e$  was the period of the modulating envelope and  $t_1 = 2\pi/\omega_1$  was the period of the "carrier" waves themselves. For all of the trials  $t_e$  was set to 15 seconds and  $t_1$  to one second. In practice (1) was programmed so as to maximize the range of the digital to analogue converter and the amplitude of the analogue signal was controlled separately by means of a graduated potentiometer. The experiment entailed passing the same waveform to the wave maker for different "gain" settings of the potentiometer and

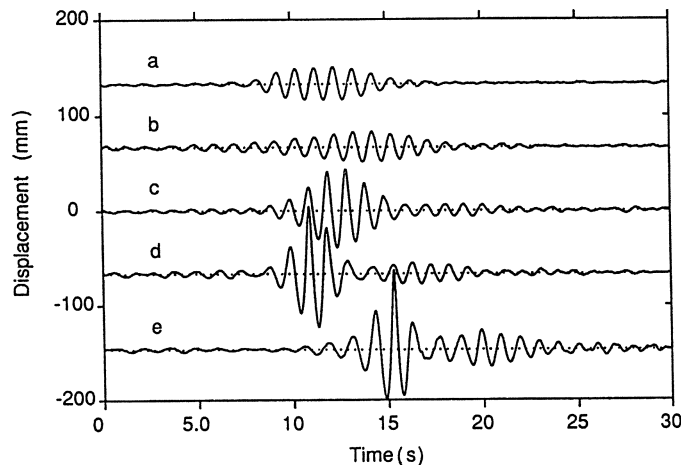


Fig.1. Time series of surface displacement:  
 (a) near probe,  $ak = 0.07$ , (b) far probe,  $ak = 0.13$ ,  
 (c) far probe,  $ak = 0.18$ , (d) far probe,  $ak = 0.21$ ,  
 (e) far probe,  $ak = 0.24$ .

recording the surface height as a function of time as the wave disturbance passed each probe.

### Results

Examples of time series recorded by the probes are shown plotted in Figure 1. For a small initial amplitude (b) the packet becomes more dispersed while for greater amplitudes (c,d,e) the disturbance forms itself into an envelope soliton followed by a dispersed tail. There is no obvious difference between (d) and (e) despite the fact that spontaneous wave breaking was observed to occur in case (e) but not in case (d).

The variance spectra of the same five time series are shown in Figure 2. The effect of the sideband instability can be clearly seen in cases (d) and (e) whereby the initial carrier frequency has been replaced by two or more sidebands. There is a noticeable difference between (d) and (e) in that there is proportionately less variance in the upper sidebands in the case, (e), for which spontaneous wave breaking had occurred.

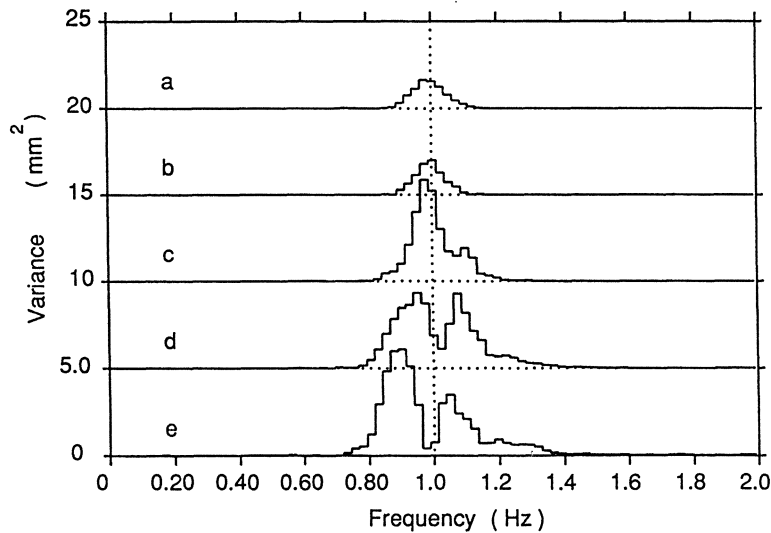


Fig.2. Variance spectra of the time series displayed in Fig.1. The zeroes are displaced for display purposes.

The results for nine different runs with varying initial steepnesses are summarised in Figure 3. A nominal initial steepness,  $ak$ , was defined as  $a_m \omega_1^2 / g$ , where  $a_m$  was the maximum excursion of the water surface measured at the first probe. The arrow indicates the interval in which spontaneous breaking commences when the initial steepness is gradually increased. Breaking was observed during all of the runs plotted to the right of the arrow. The figure shows that there was a nett loss in variance with increasing initial steepness and that this variance loss was due to losses from the upper sideband in the range of steepnesses for which breaking occurred.

### Conclusions

To first order the variance of surface height is proportional to the energy density of the wave disturbance and the missing variance can be accounted for in terms of the transfer of energy by wave breaking from the wave field into turbulence.

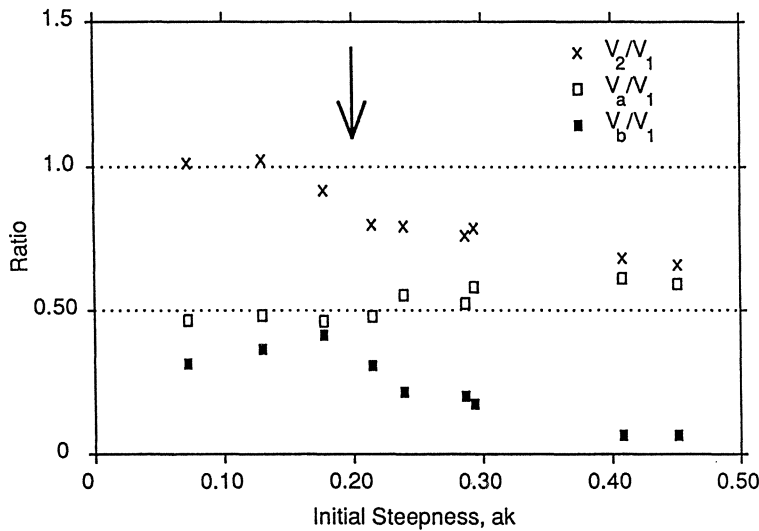


Fig.3. Ratios of far probe variances to near probe variance,  $V_1$ .  $V_2$  is the total far probe variance,  $V_a$  is the far probe variance summed over frequencies less than 1 Hz and  $V_b$  is the far probe variance summed over frequencies greater than 1 Hz.

The preferential removal of energy from the upper sidebands by this process results in a nett downward shift in the average frequency of the spectrum.

Frequency downshifting is a common phenomenon of wind seas in the open ocean. Figure 4 shows spectra (a) and (e) of Figure 2 replotted using logarithmic scales. The upper spectrum (e) shows some other features in common with wind sea spectra, viz a steep low frequency roll-off, a power law high frequency roll-off and a peak enhancement above the power law trend. This suggests that the broad features of wind sea spectra may be accounted for in terms of the sideband instability or some similar process coupled with wave breaking. The fourth order wave-wave interactions usually invoked to describe open sea spectra are certainly not applicable to the present experiment because of its two dimensional nature.

#### Acknowledgement

The author wishes to thank Dr Martin Renilson and the Australian Maritime College for use of the wave tank.

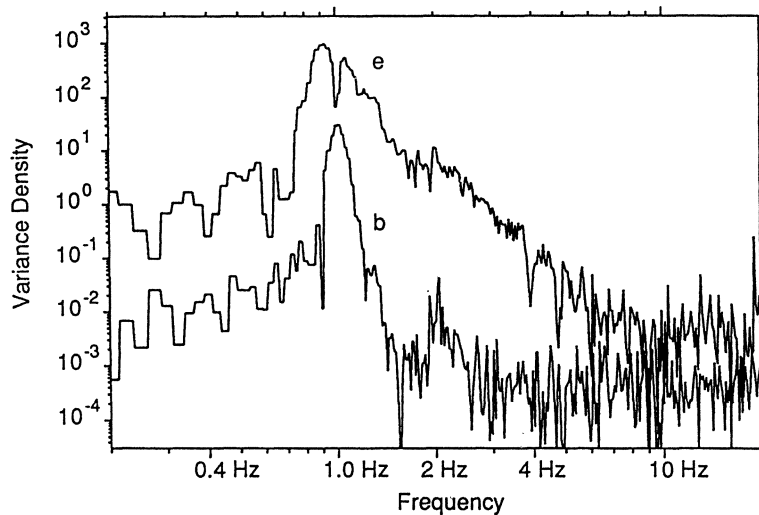


Fig. 4. The variance spectra (b) and (e) of Fig. 2 replotted with logarithmic scales. The upper curve, (e), is raised by a factor of ten for display purposes.